1704 *Chem. Mater.* **2010,** *22,* 1704–1713
DOI:10.1021/cm903497h

CHEMISTRY OF MATERIALS
Article

Tuning Ferro- and Metamagnetic Transitions in Rare-Earth Cobalt Phosphides $La_{1-x}Pr_xCo_2P_2$

Kirill Kovnir,[†] Corey M. Thompson,[†] H. D. Zhou,[‡] Christopher R. Wiebe,[§] and Michael Shatruk*,[†]

[†]*Department of Chemistry and Biochemistry, Florida State University, Tallahassee, Florida 32306,* [‡]*Department of Physics and National High Magnetic Field Laboratory, Florida State University, Tallahassee, Florida 32306, and* [§]*Department of Chemistry, University of Winnipeg, Winnipeg, Manitoba, Canada R3B 2E9*

Received October 9, 2009. Revised Manuscript Received January 11, 2010

A family of rare-earth cobalt phosphides $La_{1-x}Pr_xCo_2P_2$ ($0 \le x \le 1$) that belong to the $ThCr_2Si_2$ structure type has been prepared and characterized by structural and magnetic methods and electronic band structure calculations. All studied quaternary phases exhibit multiple magnetic transitions, leading to an observation of ferro- and metamagnetism and magnetic pole reversal. The ferromagnetic transition temperature of $LaCo_2P_2$ (132 K) increases dramatically upon substitution of Pr for La and reaches 268 K for $La_{0.25}Pr_{0.75}Co_2P_2$. This increase is accompanied by elongation of intralayer Co−Co distances. Variable temperature X-ray diffraction data revealed that temperature dependences of unit cell parameters, and, correspondingly, both intra- and interlayer Co−Co separations show anomalous changes at temperatures close to the ferromagnetic transition. The electronic structure calculations reveal a strong peak in the nonmagnetic density of states (DOS). This instability is removed in the spin-polarized DOS due to the splitting of the majority and minority spin subbands, in accord with the ferromagnetic ordering in the $[Co_2P_2]$ layer.

Introduction

Exploration of chemical factors that influence magnetic properties of solids is one of the major steps in the development of novel magnetic materials. Recent achievements in the fields of magnetic refrigerants[1−3] and FeAs-based superconductors[4,5] are excellent examples of a rational design of new materials based on understanding of their structure−property relationship. The discovery of the FeAs-based superconductors has revitalized the interest in the $ThCr_2Si_2$ structure type which includes around 1000 compounds.[6] In this structure (Figure 1), transition metal atoms (T) form planar square nets, and nonmetal atoms (X = Si, Ge, P, As) cap the centers of the squares above and below the planes in a chessboard-like fashion. The resulting $[T_2X_2]$ layers are separated by layers of rare-earth, actinide, alkali-earth, or alkali metal cations (A).

Besides superconductivity, AT_2X_2 phases exhibit a plethora of other phase transition phenomena. Thus, $SmMn_2Ge_2$ becomes ferromagnetic below 348 K and then undergoes a transition to an antiferromagnetic state at 196 K, followed by a re-entrant ferromagnetic transition at 64 K.[7] This peculiar magnetic behavior stems from the layered structure and the presence of two magnetic sublattices in these materials and was later observed for a number of rare-earth manganese germanides and silicides.[8−13]

Such sequential magnetic transitions have not been observed in isostructural phosphides, which might explain why their magnetic properties received somewhat less attention as compared to the tetrelides. Nevertheless, a survey of the known rare earth − cobalt phosphides reveals a striking difference in properties between $LaCo_2P_2$ and the other members of the series, $LnCo_2P_2$ (Ln = Ce, Pr, Nd, Sm). The former exhibits ferromagnetic ordering at 125 K,[14] while the latter order antiferromagnetically at around room temperature[15] (with the exception of the

*Corresponding author. E-mail: shatruk@chem.fsu.edu.

(1) Pecharsky, V. K.; Gschneidner, K. A.Jr. *Phys. Rev. Lett.* **1997**, *78*, 4494–4497.
(2) Tegus, O.; Brück, E.; Buschow, K. H. J.; de Boer, F. R. *Nature* **2002**, *415*, 150–152.
(3) Miller, G. J. *Chem. Soc. Rev.* **2006**, *35*, 799–813.
(4) Rotter, M.; Tegel, M.; D. Johrendt, D. *Phys. Rev. Lett.* **2008**, *101*, 107006.
(5) Johrendt, D.; Pöttgen, R. *Phys. C* **2009**, *469*, 332.
(6) Villars, P.; Calvert, L. D. *Pearson's Handbook of Crystallographic Data for Intermetallic Phases*; 2nd ed.; ASM International: Materials Park, OH, 1991.
(7) Fujii, H.; Okamoto, T.; Shigeoka, T.; Iwata, N. *Solid State Commun.* **1985**, *53*, 715–717.
(8) Duraj, M.; Duraj, R.; Szytula, A. *J. Magn. Magn. Mater.* **1989**, *79*, 61–66.
(9) Brabers, J. H. V. J.; Nolten, A. J.; Kayzel, F.; Lenczowski, S. H. J.; Buschow, K. H. J.; de Boer, F. R. *Phys. Rev. B* **1994**, *50*, 16410–16417.
(10) Morellon, L.; Algarabel, P. A.; Ibarra, M. R.; Ritter, C. *Phys. Rev. B* **1997**, *55*, 12363–12374.
(11) Wang, Y. G.; Yang, F.; Chen, C.; Tang, N.; Wang, Q. *J. Phys.: Condens. Matter* **1997**, *9*, 8539–8546.
(12) Fujiwara, T.; Fujii, H. *Physica B* **2001**, *300*, 198–214.
(13) Duman, E.; Acet, M.; Dincer, I.; Elmali, A.; Elerman, Y. *J. Magn. Magn. Mater.* **2007**, *309*, 40–53.
(14) Mörsen, E.; Mosel, B. D.; Müller-Warmuth, W.; Reehuis, M.; Jeitschko, W. *J. Phys. Chem. Solids* **1988**, *49*, 785–795.
(15) Reehuis, M.; Jeitschko, W. *J. Phys. Chem. Solids* **1990**, *51*, 961–968.

 Published on Web 01/29/2010

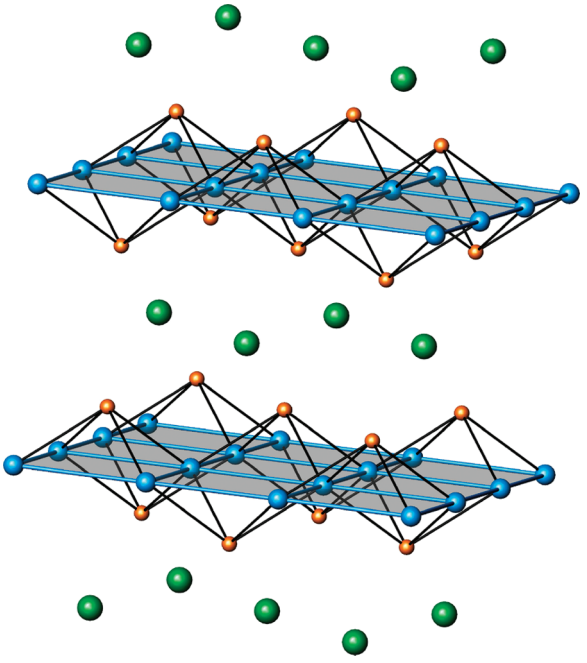

Figure 1. The crystal structure of AT_2X_2, where A = rare-earth, actinide, alkaline-earth, or alkali metal (green), T = transition metal (blue), and X = Si, Ge, P, As (orange). The planar square nets of T atoms are highlighted with gray.

Ce-containing compound that shows an antiferromagnetic transition at 440 K, purportedly due to the mixed valence of Ce). A substantial difference is also observed in the crystal structures of these compounds.[16] In $LaCo_2P_2$, the $[Co_2P_2]$ layers are far from each other, with the interlayer P−P distance of 3.16 Å indicating essentially no bonding between the phosphorus atoms. In contrast, the other $LnCo_2P_2$ structures show a weakly covalent P−P interaction at relatively short distances (compare 2.57 Å in $PrCo_2P_2$ vs 2.20 Å for the single P−P bond[17]). Thus, the drastic change in the magnetic behavior is accompanied by the formation of the P−P bonding pathway between the $[Co_2P_2]$ layers.

Based on the aforementioned differences in the properties of $LaCo_2P_2$ and the other members of the series, we hypothesized that, similarly to the tetrelides, multiple magnetic transitions can be observed for mixed quaternary phases $La_{1-x}Ln_xCo_2P_2$ (Ln = Ce, Pr, Nd, Sm). Moreover, we expect that these phosphides might exhibit importantly different magnetic behavior as compared to the tetrelides. Indeed, as demonstrated theoretically by Johrendt et al.,[18] the $[T_2X_2]$ layers become less rigid upon filling of the *d*-subband in later transition elements, and it can be anticipated that this effect also will influence the magnetic properties. To prove this hypothesis, we embarked on the study of structural, magnetic, and electronic properties of quaternary compositions $La_{1-x}Pr_xCo_2P_2$ ($0 \le x \le 1$). The choice of Pr was based on the fact that it does not exhibit mixed valence, like Ce, and therefore is the closest rare-earth neighbor of La in both the size and formal ionic charge. Thus, the use of this metal is most likely to result in an unlimited series of solid solutions, which in turn will allow a systematic assessment of magnetic behavior between the ferro- and antiferromagnetic extremes represented by $LaCo_2P_2$ and $PrCo_2P_2$, respectively. Herein, we report the preparation, characterization, and properties of these compounds, including ferromagnetic ordering that shows a strong dependence on the composition of the material, temperature- and field-driven metamagnetic transitions, and magnetic pole reversal.

Experimental Section

Starting Materials. Finely dispersed powders of lanthanum (99.9%), praseodymium (99.9%), and red phosphorus (99.999%) as well as tin shots (99.99%) were obtained from Alfa Aesar and used as received. Cobalt powder (Alfa Aesar, 99.5%) was additionally purified by heating under a flow of H_2 gas at 775 K for 5 h. All manipulations during sample preparation were carried out in an argon-filled drybox (content of O_2 < 1 ppm).

Synthesis. The preparation of rare-earth cobalt phosphides $La_{1-x}Pr_xCo_2P_2$ (x = 0, 0.12, 0.25, 0.50, 0.75, 0.88, and 1) generally followed the tin flux synthetic procedure described in the literature for $LaCo_2P_2$.[15] The starting materials were mixed in La:Pr:Co:P:Sn = $1.6(1-x)$:$1.6x$:2:2:30 ratios (total mass = 5 g) in 10 mm i.d. silica tubes, which were sealed under vacuum ($< 10^{-2}$ mbar). The mixtures were annealed at 1155 K for 10 days, then cooled down to 875 at 10 K/min, and quenched into water. To remove most of the tin flux, the obtained ingot was placed in a silica tube, along with silica wool that served as a filter. The tube was heated to 625 K for 1 h, and the melted tin flux was separated from the ingot by centrifugation. The remaining tin was removed by soaking the sample in dilute HCl (1:1 v/v) for 16 h. At this point, X-ray quality single crystals were selected from the sample. The phase purity of bulk products obtained by the described synthetic procedure was confirmed by powder X-ray diffraction.

Physical Measurements. Powder X-ray diffraction was performed on a Rigaku DMAX 300 Ultima III powder X-ray diffractometer using CuKα radiation (λ = 1.54185 Å) and Ge as an internal standard. The unit cell parameters were calculated by least-squares fitting with the WinCSD software package.[19] Elemental analysis of select single crystals was carried out on a JEOL 5900 scanning electron microscope with an energy-dispersive X-ray (EDX) microanalysis. Magnetic measurements were performed on polycrystalline samples with a Quantum Design SQUID magnetometer MPMS-XL. DC magnetic susceptibility measurements were carried out in an applied field of 0.01 T in the 1.8−350 K range. Magnetization and hysteresis were measured with the magnetic field varying from 0 to 7 T. To determine the critical field for the metamagnetic transition, the AC magnetic susceptibility was measured at 1 Hz frequency and $3 \cdot 10^{-4}$ T amplitude of the AC field under a DC bias field varied from 0 to 7 T.

Single Crystal X-ray Diffraction. In a typical room-temperature experiment, a single crystal of $La_{1-x}Pr_xCo_2P_2$ ($0 < x < 1$)

(16) Jeitschko, W.; Meisen, U.; Möller, M. H.; Reehuis, M. *Z. Anorg. Allg. Chem.* **1985**, *527*, 73–84.
(17) Von Schnering, H. G.; Hönle, W. *Chem. Rev.* **1988**, *88*, 243–273. Shatruk, M. M.; Kovnir, K. A.; Shevelkov, A. V.; Popovkin, B. A. *Angew. Chem., Int. Ed.* **2000**, *39*, 2508–2509.
(18) Johrendt, D.; Felser, C.; Jepsen, O.; Andersen, O. K.; Mewis, A.; Rouxel, J. *J. Solid State Chem.* **1997**, *130*, 254–265.
(19) Akselrud, L. G.; Zavalii, P. Y.; Grin, Y.; Pecharski, V. K.; Baumgartner, B.; Woelfel, E. *Mater. Sci. Forum* **1993**, *133−136*, 335–340.

Table 1. Data Collection and Structure Refinement Parameters for $La_{1-x}Pr_xCo_2P_2$[a]

composition	$La_{0.88}Pr_{0.12}Co_2P_2$	$La_{0.75}Pr_{0.25}Co_2P_2$	$La_{0.5}Pr_{0.5}Co_2P_2$	$La_{0.25}Pr_{0.75}Co_2P_2$	$La_{0.12}Pr_{0.88}Co_2P_2$
Pr content (x)					
- from EDX	0.07(5)	0.16(5)	0.47(5)	0.74(5)	0.89(5)
- refined	not refined	0.19(5)	0.50(6)	not refined	not refined
crystal system			*tetragonal*		
space group			*I*4/*mmm* (*no. 139*)		
temperature			293 K		
unit cell, Å	a = 3.8288(1)	a = 3.8260(1)	a = 3.8366(1)	a = 3.9017(2)	a = 3.9065(1)
	c = 10.8863(2)	c = 10.9031(3)	c = 10.6319(2)	c = 9.9438(4)	c = 9.8140(3)
V, Å^3	159.590(7)	159.603(7)	156.496(6)	151.38(1)	149.769(7)
Z			2		
λ, Å			Mo$K\alpha$, 0.71073		
ρ_{calc}, g cm^{-3}	6.638	6.640	6.785	7.025	7.106
μ, mm^{-1}	24.347	24.486	25.547	26.906	27.446
$2\theta_{max}$	80	92.6	80	80	80
refl. collected	1392	1693	1052	1088	1013
R_{int}	0.023	0.014	0.029	0.022	0.019
independ. refls.	176	242	168	167	160
param. refined	9	10	10	9	9
R_1, wR_2 [$F_o > 4\sigma F_o$]	0.021, 0.053	0.012, 0.031	0.015, 0.032	0.016, 0.039	0.016, 0.034
diff. peak and hole, e/Å^3	2.14 and −2.41	1.25 and −1.04	0.80 and −1.75	1.25 and −1.78	0.97 and −2.88
goodness-of-fit	1.36	1.28	1.15	1.23	1.32

[a] Further details of the crystal structure determination may be obtained from Fachinformationszentrum Karlsruhe, D-76344 Eggenstein-Leopoldshafen, Germany, on quoting depository numbers CSD-421016 to CSD-421025.

was glued with epoxy cement on the tip of a quartz fiber and mounted on a goniometer head of a Bruker AXS SMART diffractometer with an APEX-II CCD detector. The same crystal was later used for low-temperature experiments. The crystal was suspended in Parathone-N oil (Hampton Research) and mounted on a cryoloop which was placed in an N_2 cold stream, cooled down at 5 K/min, and allowed to equilibrate at the desired temperature for at least 1 h prior to the data collection.

In general, the data sets were recorded as ω-scans at 0.3° stepwidth and integrated with the Bruker SAINT software package.[20] All the data sets were indexed in the tetragonal body-centered unit cell. The only systematic extinctions observed corresponded to the *I*-centered lattice. In most of the experiments, an analytical absorption correction was applied using face-indexing of the crystal. Whenever an accurate face-indexing was impossible due to poor visibility of crystal faces, the absorption correction was based on fitting a function to the empirical transmission surface as sampled by multiple equivalent measurements (SADABS).[21] Solution and refinement of the crystal structures was carried out using the SHELX suite of programs.[22] The structures were solved in the *I*4/*mmm* space group (no. 139), and the final refinement was performed with anisotropic atomic displacement parameters for all atoms. A summary of pertinent information relating to unit cell parameters, data collection, and refinements is provided in Table 1. The details of the crystal structure determination are described in the Results and Discussion section.

Variable Temperature Powder X-ray Diffraction. Data were collected on an original setup based on a Huber imaging plate Guinier camera 670 using Cu$K\alpha_1$ radiation (λ = 1.54060 Å) with a Ge crystal monochromator. X-ray patterns were acquired at 0.005° resolution in the temperature range of 10−300 K by employing a closed-cycle He refrigeration system. The unit cell parameters were calculated by the refinement of a set of 12 reflections common to all samples, using least-squares fitting by the WinCSD software package.[19]

Quantum-Chemical Calculations. Band structure calculations were performed with the tight binding-linear muffin tin orbitals-atomic sphere approximation (TB-LMTO-ASA) software package.[23] The von Barth−Hedin exchange-correlation potential was employed for the local density approximation (LDA) calculations.[24] The radial scalar-relativistic Dirac equation was solved to obtain the partial waves. The experimentally determined room temperature crystal structure parameters (unit cell dimensions and atomic coordinates) were used in the calculations. No empty spheres had to be added. The calculations were made for 21952 (28 × 28 × 28) *k*-points in the Brillouin zone (BZ). Integration over the Brillouin zone was carried out by the tetrahedron method.[25] The basis set contained La(6s, 5d, 4f), Co(4s, 4p, 3d), and P(3s, 3p) orbitals, with the La(6p) and P(3d) functions being downfolded.[26]

Results and Discussion

Synthesis. As shown earlier by Jeitschko et al.,[15] a 20−30% excess of rare-earth metal is necessary to obtain single-phase $LnCo_2P_2$ products by annealing in tin flux. At the stoichiometric 1:2:2 ratio, the formation of Co- and P-rich phases is observed, but the excess of rare-earth metal shifts the equilibrium toward the formation of the desired $LnCo_2P_2$ phase. In our experiments, we confirmed this observation and determined that the ratio Ln:Co:P:Sn = 1.6:2:2:30 provides the best results. Elimination of tin matrix by high-temperature centrifugation and dissolution in HCl (1:1 v/v) produces single-phase $La_{1-x}Pr_xCo_2P_2$ samples that consist of relatively small crystals (~0.1 mm). For $x \leq 0.5$, the crystals formed as square plates growing perpendicular to the [001] direction

(20) *SMART and SAINT*; Bruker AXS Inc.: Madison, WI, USA, 2007.
(21) Sheldrick, G. M. *SADABS*; University of Göttingen: Göttingen, Germany, 1996.
(22) Sheldrick, G. M. *Acta Crystallogr., Sect. A: Found. Crystallogr.* **2008**, *A64*, 112–122.
(23) Jepsen, O.; Burkhardt, A.; Andersen, O. K. *The program TB-LMTO-ASA. Version 4.7*; Max-Planck-Institut für Festkorperforschung: Stuttgart, 1999.
(24) Von Barth, U.; Hedin, L. *J. Phys. C* **1972**, *5*, 1629–1642.
(25) Blöchl, P. E.; Jepsen, O.; Andersen, O. K. *Phys. Rev. B* **1994**, *49*, 16223–16233.
(26) Lambrecht, W. R. L.; Andersen, O. K. *Phys. Rev. B* **1986**, *34*, 2439–2449.

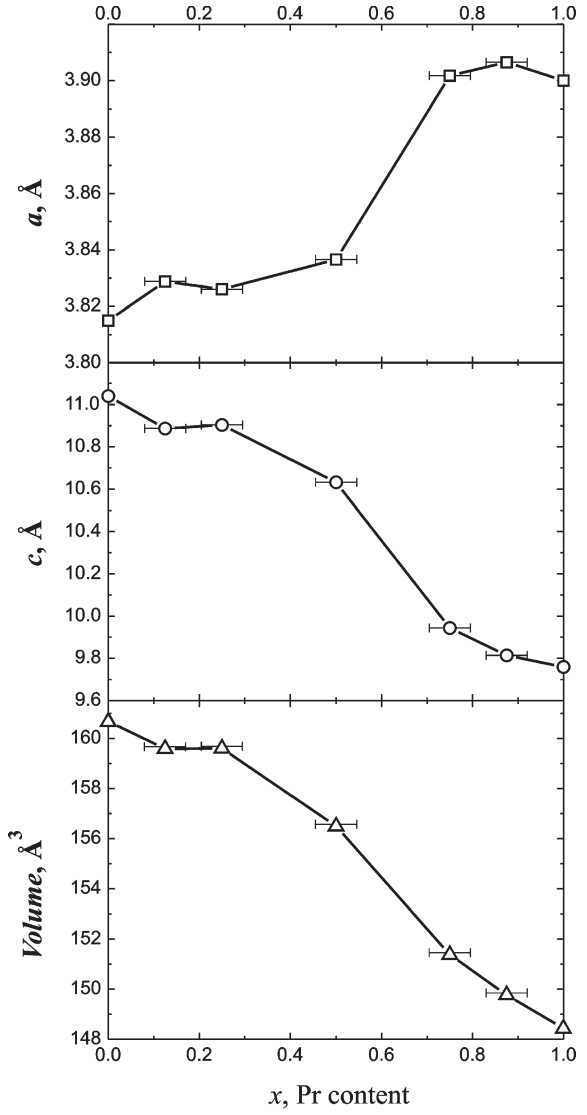

Figure 2. Unit cell parameters and volume of $La_{1-x}Pr_xCo_2P_2$ as a function of Pr content, x. The standard deviations for unit cell parameters and volume are smaller than the symbol size.

(Figure S1), which emphasizes the layered structure of these phases. For higher values of x, the crystals were shaped as truncated square pyramids. X-ray powder diffraction analysis confirmed the phase purity of the samples. Unit cell parameters are in good agreement with those obtained from single-crystal experiments.

The EDX analysis reveals that the La/Pr ratio in the obtained crystals agrees well with the nominal composition used for the sample preparation (Table 1). The relatively high estimated standard deviations (esd) are explained by the overlap of La and Pr lines in the EDX spectrum and nonideal orientation of the crystals with respect to the electron beam. For the samples with $x < 0.5$, a slightly lower Pr content is detected, which nonetheless matches the nominal composition within the esd. Therefore, in the following discussion, the nominal Pr content will be used.

Crystal Structures. The structures of $La_{1-x}Pr_xCo_2P_2$ were determined by single-crystal X-ray diffraction (Table 1). As expected, all the $La_{1-x}Pr_xCo_2P_2$ phases

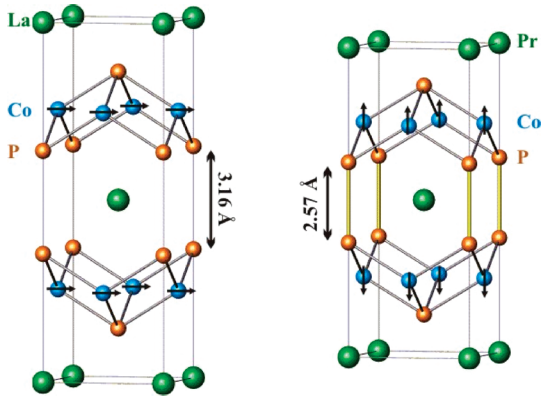

Figure 3. Magnetic ordering in $LaCo_2P_2$ (left) and $PrCo_2P_2$ (right). Black arrows indicate spin ordering below T_C and T_N, respectively.

crystallize in the tetragonal space group $I4/mmm$ and are isostructural with $LaCo_2P_2$. The La and Pr atoms occupy a mixed position ($2a$) in the origin of the unit cell. The quality of single crystals with $x = 0.12$, 0.75, and 0.88 was not sufficient for a reliable refinement of the La:Pr ratio due to the similarity of the La and Pr scattering factors and relatively small concentration of one of the metals. Therefore, in these crystal structures, the La and Pr site occupancy factors (s.o.f.'s) were fixed to the nominal sample compositions, since they agree well with the results of EDX. For the crystal structures with $x = 0.25$ and 0.50, the s.o.f.'s of La and Pr were refined with the constraints of 100% total occupancy of the $2a$ position and equal atomic displacement parameters for both atoms. The refinement resulted in s.o.f.(Pr) = 0.19(5) and 0.50(6) for $x = 0.25$ and $x = 0.50$, respectively, which also agrees with the EDX results.

The structure of $La_{1-x}Pr_xCo_2P_2$ ($0 \le x \le 1$) consists of alternating layers of $[Co_2P_2]$ and rare-earth cations (Figure 1). In the $[Co_2P_2]$ layer, the Co atoms form a planar square net with $d(Co-Co) = a/\sqrt{2}$, while the P atoms cap the centers of one-half of the squares on each side of the net. The interlayer distance between P atoms is not directly proportional to the unit cell parameter c, since these atoms occupy the special position $4e$ (0,0,z) with a variable z. The parameter a increases with increasing Pr content x, with the simultaneous decrease of the parameter c. It must be noted, however, that the relative change in c is much larger than the change in a, which results in the overall reduction in the unit cell volume with increasing x (Figure 2).

Magnetic Properties. Earlier neutron diffraction studies of the magnetic structures of $LaCo_2P_2$ and $PrCo_2P_2$ revealed that Co magnetic moments are ordered ferromagnetically within each $[Co_2P_2]$ layer in both compounds (Figure 3).[27,28] This results in ferromagnetic ordering in $LaCo_2P_2$ at $T_C = 125$ K. In $PrCo_2P_2$, however, the adjacent $[Co_2P_2]$ layers are coupled

(27) Reehuis, M.; Ritter, C.; Ballou, R.; Jeitschko, W. *J. Magn. Magn. Mater.* **1994**, *138*, 85–93.
(28) (a) Reehuis, M.; Brown, P. J.; Jeitschko, W.; Möller, M. H.; Vomhof, T. *J. Phys. Chem. Solids* **1993**, *54*, 469–475. (b) Reehuis, M.; Jeitschko, W.; Kotzyba, G.; Zimmer, B.; Hu, X. *J. Alloys Compd.* **1998**, *266*, 54–60.

Table 2. Magnetic Properties of $La_{1-x}Pr_xCo_2P_2$

Pr content, x	T_C, K	T_N, K[a]	T'_N, K[a]	θ, K	μ_{eff} per formula unit	μ_{eff} (Co)[b]
0[c]	132(1)	–	–	135(1)	2.22(1)	1.57(1)
	125			*137*	*2.04*	*1.44*
0.12	150(2)	52(3)	–	157(1)	2.27(1)	1.34(1)
0.25	160(2)	78(3)	–	158(1)	2.64(2)	1.37(2)
0.5	200(2)	55(3)	–	178(2)	3.07(2)	0.23(2)
0.75	268(2)	7(1)[d]	–	273(2)	3.35(2)	0.90(2)
0.88	250(2)	17(1)[d]	305(1)	–	–	–
1[c]	–	–	303(1), *304*	–	–	

[a] T_N corresponds to the order−order (metamagnetic) transition, while T'_N designates the disorder−order transition at higher temperature (see the text). [b] The magnetic moment per Co atom was calculated by subtracting the theoretically calculated contribution of Pr^{3+} (μ_{eff} = 3.58 per Pr^{3+} ion) from the total magnetic moment calculated from the Curie−Weiss law in the paramagnetic regime.[30] [c] The literature data for $LaCo_2P_2$[14] and $PrCo_2P_2$[15] are italicized. [d] The values refer to the low-temperature ordering of the Pr sublattice, T_{Pr} (see the text).

antiferromagnetically, and the compound is an antiferromagnet with T_N = 304 K. Our results for samples with x = 0 and x = 1 are in good agreement with the reported data (Table 2); $LaCo_2P_2$ orders ferromagnetically at 132 K, and $PrCo_2P_2$ orders antiferromagnetically at 303 K (the slight deviation from the literature data is probably due to different measurement techniques). In the case of $LaCo_2P_2$, we performed a careful study of magnetization around the ordering temperature, and an analysis of the Arrott plot[29] indicated T_C = 132(1) K as an isotherm at which the change in the curvature of the M^2 vs M/H dependence is observed (Figure S2).

The quaternary phases $La_{1-x}Pr_xCo_2P_2$ exhibit more complicated magnetic behavior, with at least two discernible phase transitions in each case (Table 2). All the samples, except for the one with x = 0.88, are paramagnetic at 300 K. Asymptotic Curie temperatures θ obtained from Curie−Weiss fitting of the high-temperature part of $1/\chi$ vs T plots are positive, indicating ferromagnetic nearest-neighbor interactions within the $[Co_2P_2]$ layer. Upon decreasing the temperature, a ferromagnetic transition is observed (Figure 4), which is assigned to the ordering of Co magnetic moments. This conclusion is supported by the ferromagnetism of $LaCo_2P_2$ and the fact that the other $LnCo_2P_2$ phases show no ordering in the rare-earth sublattice above 100 K.[28] Remarkably, the ferromagnetic ordering temperature (T_C) of $La_{1-x}Pr_xCo_2P_2$ increases dramatically upon substitution of Pr for La (from 132 K at x = 0 to 268 K at x = 0.75). This is in drastic contrast to the magnetic behavior of $LnMn_2Si_2$ phases, in which the ferromagnetic ordering temperature remains nearly unaffected by isoelectronic substitutions into the rare-earth sublattice (vide infra).[13] A study of magnetic behavior of $La_{1-x}Pr_xCo_2P_2$ (x = 0, 0.12, 0.25, and 0.50) in a variable magnetic field at 100 K showed that these materials behave as soft ferromagnets. The hysteresis loop slightly widens for samples with higher Pr content (Figure S3).

Introduction of Pr into the $LaCo_2P_2$ structure dramatically modifies the low-temperature magnetic behavior. Phases $La_{1-x}Pr_xCo_2P_2$ with x = 0.12, 0.25, and 0.50

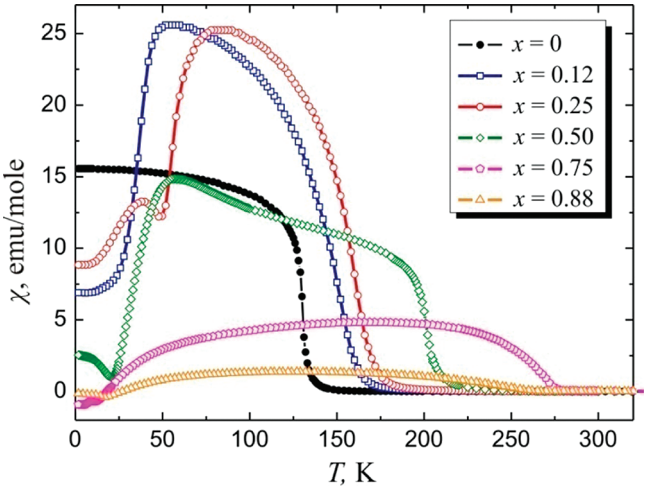

Figure 4. Temperature dependence of magnetic susceptibilities of $La_{1-x}Pr_xCo_2P_2$ measured in the DC applied magnetic field of 0.01 T.

exhibit a metamagnetic transition[31] which manifests itself as an abrupt drop in magnetic susceptibility below 52 K, 78 K, and 55 K, respectively. Since the character of this transition appears to be similar for these three phases (x = 0.12, 0.25, and 0.50), it can be attributed to antiferromagnetic coupling between the ferromagnetically ordered $[Co_2P_2]$ layers. The fact that the magnetization exhibits quite high residual value in the bottom of the transition indicates that the actual magnetic structure might be more complex and involve canted or helical ordered states.[32] Note that the participation of Pr magnetic moments in this transition cannot be ruled out. On the one hand, it was demonstrated by neutron diffraction studies that in $PrCo_2P_2$ the Pr spins are disordered above 30 K.[28]

(29) Arrott, A. *Phys. Rev.* **1957**, *108*, 1394–1396.
(30) The study of an isostructural compound, $PrFe_2P_2$, in which Fe atoms do not carry magnetic moments, confirmed that the Pr paramagnetic contribution is close to the theoretically calculated value.[15]
(31) The term "metamagnetic" is conventionally used to describe an abrupt field-induced increase in magnetization associated with the transition from antiferromagnetic to ferromagnetic state. Nevertheless, a similar effect can be achieved by varying the temperature, in which case it might be classified as temperature-induced metamagnetic transition (see, for example, Brabers, J. H. V. J.; Nolten, A. J.; Kayzel, F.; Lenczowski, S. H. J.; Buschow, K. H. J.; de Boer, F. R. *Phys. Rev. B* **1994**, *50*, 16410–16417. Palstra, T. T. M.; Werij, H. G. C.; Nieuwenhuys, G. J.; Mydosh, J. A.; de Boer, F. R.; Buschow, K. H. J. *J. Phys. F* **1984**, *14*, 1961–1966. Gaidukova, I. Yu.; Gratz, E.; Markosyan, A. S.; Petropavlovsky, A. B.; Rodimin, V. E. *Physica B* **2005**, *355*, 54–58. Reich, W.; Cofta, H.; Michalski, K. J. *Phys. Lett. A* **1979**, *74*, 119–120). For brevity, we are using the term "metamagnetic" for both field- and temperature-induced antiferromagnetic-ferromagnetic transitions. .
(32) Venturini, G.; Welter, R.; Ressouche, E.; Malaman, B. *J. Alloys Compd.* **1994**, *210*, 213–220.

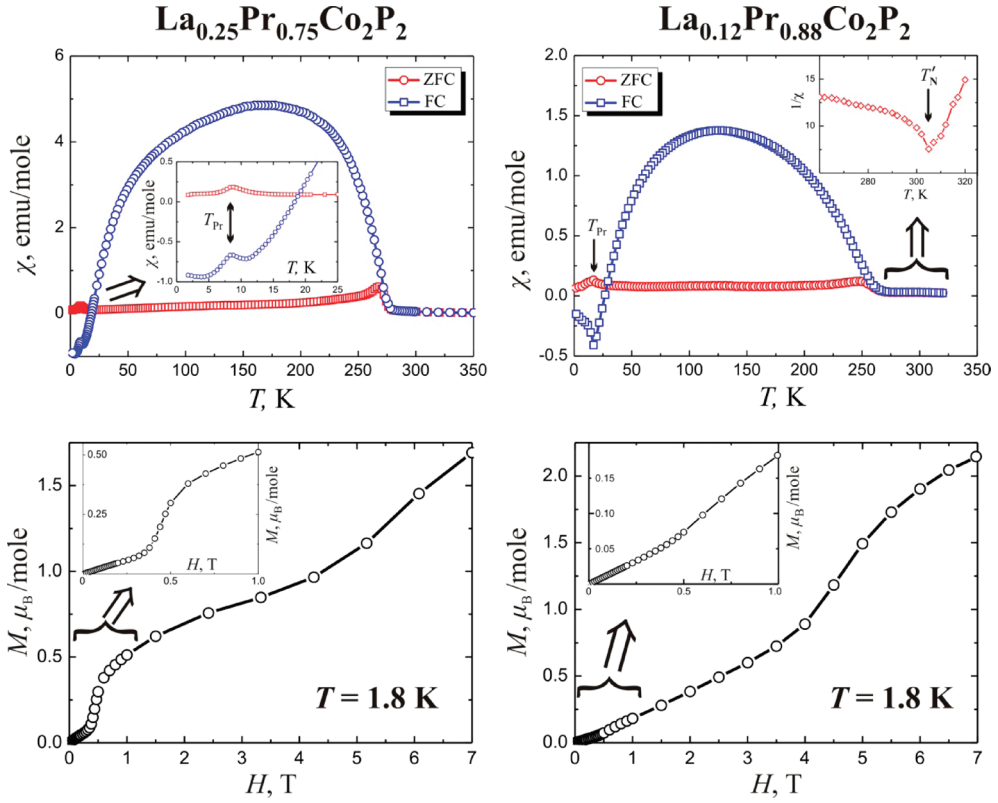

Figure 5. Temperature dependence of zero-field cooled and field cooled magnetic susceptibilities (top) and field dependence of magnetization (bottom) for $La_{1-x}Pr_xCo_2P_2$ ($x = 0.75$, left; $x = 0.88$, right). Each inset shows a magnified portion of the corresponding curve.

On the other hand, in $NdCo_2P_2$, a gradual ordering of Nd spins was observed below 100 K, presumably induced by the Co magnetic moments.[28] Thus, neutron diffraction studies of the $La_{1-x}Pr_xCo_2P_2$ phases are necessary to conclusively establish the role of the rare-earth sublattice in the observed low-temperature behavior. These studies will also shed light on the nature of the additional magnetic transitions observed for samples with $x = 0.25$ and 0.50 at 38 and 21 K, respectively (Figure 4). Such a transition is not observed for the sample with the smaller Pr content ($x = 0.12$), which suggests the participation of Pr magnetic moments.

With increasing Pr content in $La_{1-x}Pr_xCo_2P_2$, the magnetic moment per Co atom decreases (Table 2). In the phases with $x = 0.75$ and 0.88, the ferromagnetic ordering temperature further increases, although the transition becomes less abrupt (Figure 5). Moreover, the phase with $x = 0.88$ shows a weak antiferromagnetic ordering (disorder−order transition) at 305 K.[33] In contrast to the phases with the lower Pr content, no discernible metamagnetic transition can be observed for $La_{0.25}Pr_{0.75}Co_2P_2$ and $La_{0.12}Pr_{0.88}Co_2P_2$ at moderate temperatures. Only a gradual decrease in the susceptibility is observed below 100−150 K, which suggests that the competition between ferro- and antiferromagnetic interactions in these phases is much stronger.

Furthermore, the samples with $x = 0.75$ and 0.88 exhibit an interesting behavior not observed in the other phases of the $La_{1-x}Pr_xCo_2P_2$ series, as for both of them the magnetization changes sign at lower temperatures. This is due to the increased magnetic contribution from Pr, which, when coupled antiferromagnetically with respect to the Co sublattice, results in the reversal of the total magnetization at the compensation point (18 K for $x = 0.75$ and 27 K for $x = 0.88$). Such magnetic pole reversal was predicted by Néel[34] and observed, for example, in some rare-earth garnet ferrites[35] and oxalato- and cyano-bridged coordination polymers.[36−38] To the best of our knowledge, this is the first reported example of such behavior in materials with the $ThCr_2Si_2$-type structure. Since these solids contain two magnetic sublattices that are often coupled antiferromagnetically with respect to each other,[39] it can be expected that other cases of magnetic pole reversal can be found among them.

Magnetic behavior of both $La_{0.25}Pr_{0.75}Co_2P_2$ and $La_{0.12}Pr_{0.88}Co_2P_2$ is characterized by a significant magnetic anisotropy of the Co sublattice, as evidenced by the large divergence of the zero-field cooled vs field cooled susceptibility curves (Figure 5, top). This is consistent

(33) The transition due to the admixture of $PrCo_2P_2$ can be ruled out, as the sample with $x = 0.88$ was shown to be phase-pure by X-ray powder diffraction and the magnitude of the observed transition cannot be justified by a small (< 5%) admixture of $PrCo_2P_2$.

(34) Néel, L. *Ann. Phys.* **1948**, *3*, 137–198.
(35) Gorter, E. W. *Philips Res. Rep.* **1954**, *9*, 403–443. Pauthenet, R. *J. Appl. Phys.* **1958**, *29*, 253–255.
(36) Mathonière, C.; Nuttall, C. J.; Carling, S. G.; Day, P. *Inorg. Chem.* **1996**, *35*, 1201–1206.
(37) Ohkoshi, S. i.; Hashimoto, K. *J. Am. Chem. Soc.* **1999**, *121*, 10591–10597. Ohkoshi, S. i.; Arai, K. i.; Sato, Y.; Hashimoto, K. *Nat. Mater.* **2004**, *3*, 857–861.
(38) Egan, L.; Kamenev, K.; Papanikolaou, D.; Takabayashi, Y.; Margadonna, S. *J. Am. Chem. Soc.* **2006**, *128*, 6034–6035.
(39) Brooks, M. S. S.; Johansson, B. *Handb. Magn. Mater.* **1993**, *7*, 139–230.

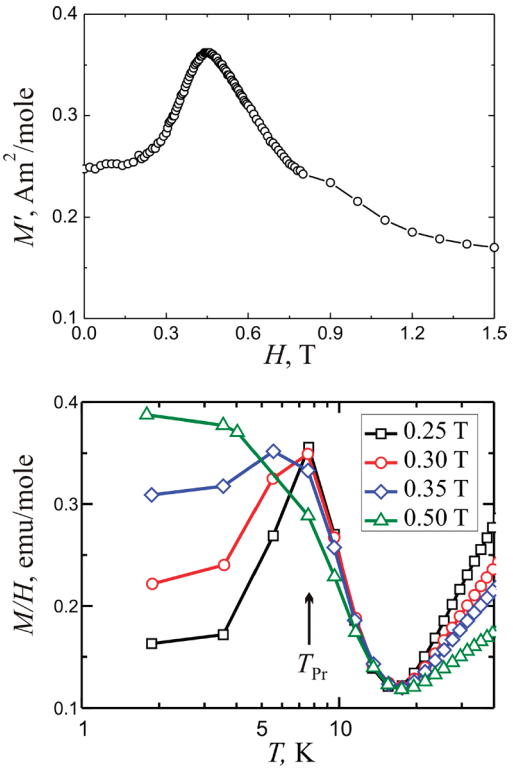

Figure 6. Metamagnetic behavior of $La_{0.25}Pr_{0.75}Co_2P_2$: dependence of the in-phase component of AC magnetization on the applied DC magnetic field (top) and temperature dependence of M/H in various applied DC fields (bottom).

with the observation of the compensation points for these phases, as magnetic anisotropy of one of the sublattices is a necessary condition for such behavior. Below the compensation point, $La_{0.25}Pr_{0.75}Co_2P_2$ and $La_{0.12}Pr_{0.88}Co_2P_2$ exhibit antiferromagnetic phase transitions at 7 and 17 K, respectively (Figure 5, top, insets), most probably due to the ordering of Pr magnetic moments.

The field dependence of magnetization of $La_{0.18}Pr_{0.88}Co_2P_2$ measured at 1.8 K is characteristic of an antiferromagnet up to 4 T, at which point an onset of a metamagnetic transition is seen, with the critical field around 4.5 T (Figure 5, bottom). An examination of the field-dependent magnetization of $La_{0.25}Pr_{0.75}Co_2P_2$ at 1.8 K reveals antiferromagnetic behavior at low field, followed by a field-induced metamagnetic transition around 0.4 T. The AC magnetization measured as a function of applied DC field gives the value of critical field $H_{cr} = 0.45(1)$ T as the maximum of the χ' vs H curve (Figure 6). Another metamagnetic transition is observed at much higher fields (~6 T), but the accurate determination of the critical field for this transition was hampered by instrumental limitations. Based on the observed field-dependent magnetic behavior, the low-field metamagnetic transition is assigned to the reorientation of Pr spins, while the high-field metamagnetic transition is due to the reorientation of Co spins, which is consistent with the high magnetic anisotropy observed for the Co sublattice.

Variable Temperature Powder X-ray Diffraction. To study correlations between the magnetic behavior and structural characteristics of $La_{1-x}Pr_xCo_2P_2$, high accuracy unit cell parameters were refined from the powder X-ray diffraction patterns collected at variable temperature (Figure 7). An examination of unit cell parameters of samples with $x = 0.25$ and 0.50 reveals that the unit cell volume decreases as the temperature is lowered from 300 K, although a and c change in the opposite directions. This is similar to the alteration in unit cell parameters associated with the change of the Pr content, x (Figure 2). In the vicinity of the ferromagnetic transition, the changes in the unit cell parameters reverse, as a begins to increase and c decreases. The volume of the unit cell, however, continues to decrease. For $La_{0.75}Pr_{0.25}Co_2P_2$, these trends remain essentially the same as the temperature decreases from $T_C = 160$ to 10 K. On the other hand, for $La_{0.50}Pr_{0.50}Co_2P_2$, the changes in unit cell parameters again reverse at the antiferromagnetic transition temperature, and, importantly, an anomaly is observed in the unit cell volume. The observed behavior indicates that ferromagnetic ordering in the $La_{1-x}Pr_xCo_2P_2$ phases favors longer intralayer Co−Co distances (vide infra).

We also carried out an analogous study on single crystals of phases with $x = 0.25$, 0.5, and 0.88. For each sample, the variable temperature crystal structure determination was performed on the same crystal. The observed changes in unit cell parameters and volume parallel those found from the powder diffraction data (Table S1).

Comparison of Co- and Mn-Containing Phases. The rare-earth cobalt phosphides behave quite differently from the extensively investigated rare-earth manganese silicides and germanides,[7−13] both in the structural and magnetic sense. To eliminate factors associated with the nature of the rare earth ions, we compare the behavior of $La_{1-x}Pr_xCo_2P_2$ and $La_{1-x}Pr_xMn_2Si_2$ phases. In phosphides, the temperature of the ferromagnetic transition changes from 132 K at $x = 0$ to 268 K at $x = 0.75$, while the metamagnetic transition is much less affected by the changes in x (Table 2). On the other hand, in silicides, the ferromagnetic ordering temperature remains essentially unaffected by the substitution in the rare earth sublattice ($T_C \sim 300$ K), but the metamagnetic transition shifts from ~170 K at $x = 0.40$ to ~260 at $x = 0.50$.[13] In contrast to phosphides, in which the consecutive magnetic transitions are observed for all but limiting values of x, $La_{1-x}Pr_xMn_2Si_2$ phases exhibit such behavior only for a very narrow composition range ($x = 0.40 \div 0.50$). From the structural viewpoint, the phosphides are also more tolerant to the changes that take place upon isoelectronic substitution into the rare-earth sublattice.[40] The lower rigidity of the $[T_2X_2]$ layer in Co- vs Mn-containing phases is justified by the earlier theoretical investigations of the $ThCr_2Si_2$-type structures.[18] Our results provide the experimental evidence that this structural effect is also reflected in the magnetic behavior of $La_{1-x}Pr_xCo_2P_2$ phases.

(40) Upon going from $LaCo_2P_2$ to $PrCo_2P_2$, the parameter c decreases by ~12% and the parameter a increases by ~2%. On the other hand, the change in the unit cell parameters between $LaMn_2Si_2$ and $PrMn_2Si_2$ is only about 2% for a and less than 0.5% for c, with both parameters decreasing.

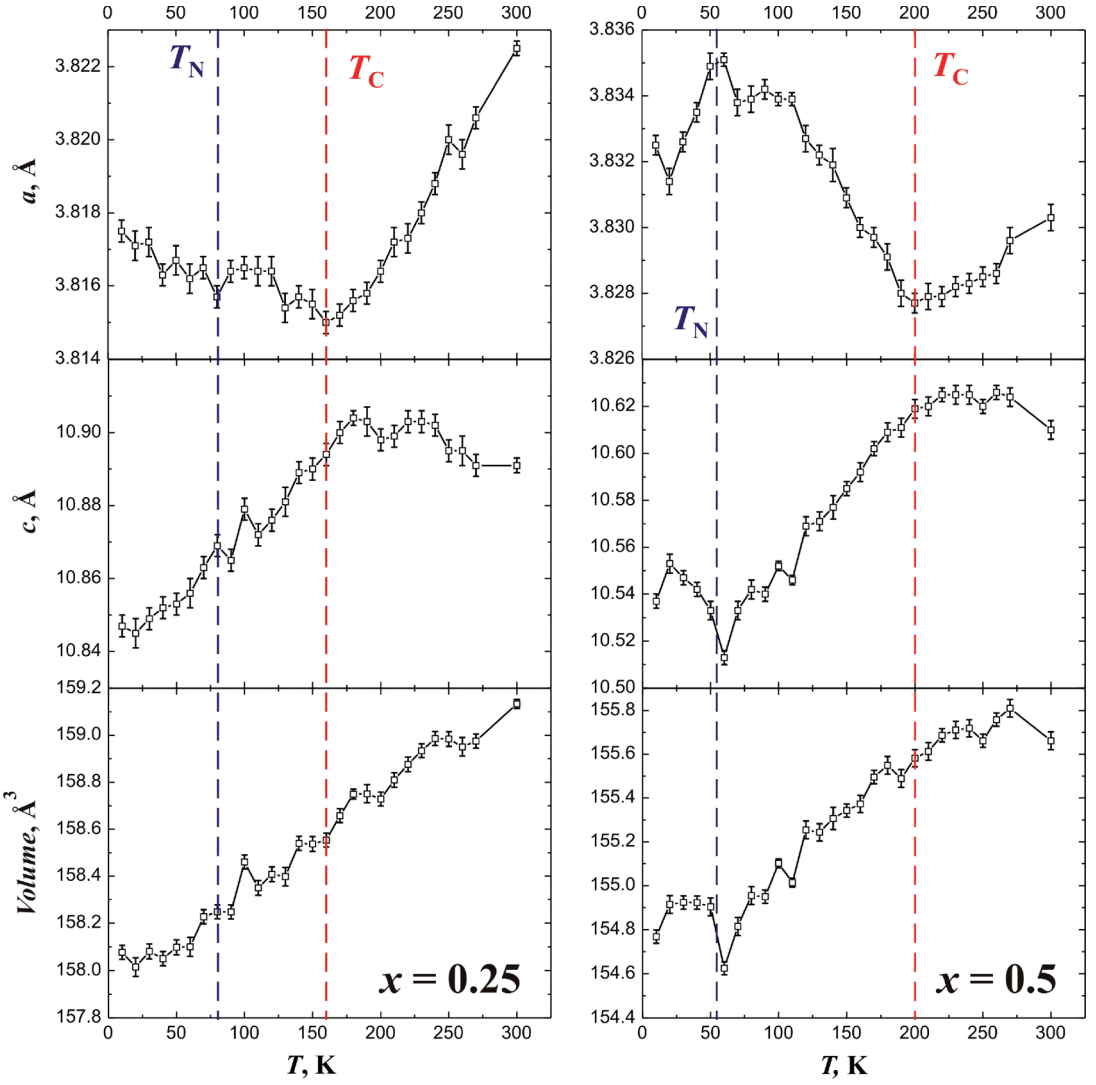

Figure 7. Temperature dependence of the unit cell parameters and volume of $La_{1-x}Pr_xCo_2P_2$: $x = 0.25$ (left) and $x = 0.5$ (right). T_C and T_N obtained from magnetic measurements are shown with red and blue dashed lines, respectively.

Electronic Structure

The electronic structure of the $ThCr_2Si_2$-type phosphides was rationalized by Hoffmann and Zheng based on theoretical calculations using the extended Hückel method.[41] According to their analysis, the formation of the P−P bond depends on the population of the transition metal's 3*d* band and its energy with respect to the σ and σ^* orbitals of the P−P interaction. This approach, however, was later criticized by Johrendt et al.[18] who demonstrated that the situation is more complex and involves the influence of the intralayer T-P and T-T interactions on the P−P bonding. Importantly, these authors arrived at the conclusion about the lower rigidity of the $[T_2X_2]$ layer for metals with the higher *d*-band occupation. As seen in the current study, this effect also translates to the magnetic behavior of the $La_{1-x}Pr_xCo_2P_2$ phases.

Both the ferromagnetic ordering temperature and the intralayer Co−Co distance increase with the Pr content (Figure 8). The correlation between the Co−Co separation and ferromagnetic transition was also conjectured from the temperature dependence of the unit cell parameters (Figure 7). In order to understand this behavior, the spin-polarized band structure of these phases was investigated.

The electronic structures were calculated by the tight binding-linear muffin tin orbitals-atomic sphere approximation (TB-LMTO-ASA) method.[42] The LMTO approach is known to underestimate correlation energies of the 4*f* states in lanthanides, especially in the case of significant spin−orbit coupling. Nevertheless, it was demonstrated that LMTO produces sufficiently accurate results for empty f^0 (La), half-filled f^7 (Gd), and completely filled f^{14} (Lu) shells where spin−orbit coupling is not present.[18,43,44] Therefore, in all the calculations, the (2*a*) position at the origin of the unit cell was set

(41) Hoffmann, R.; Zheng, C. *J. Phys. Chem.* **1985**, *89*, 4175–4181. *Chemistry, Structure, and Bonding of Zintl Phases and Ions*; Kauzlarich, S. M., Ed.; VCH: New York, 1996.

(42) Andersen, O. K.; Pawlowska, Z.; Jepsen, O. *Phys. Rev. B* **1986**, *34*, 5253–5269.

(43) Skriver, H. L.; Andersen, O. K.; Johansson, B. *Phys. Rev. Lett.* **1980**, *44*, 1230–1233.

(44) Svitlyk, V.; Miller, G. J.; Mozharivskyj, Y. *J. Am. Chem. Soc.* **2009**, *131*, 2367–2374.

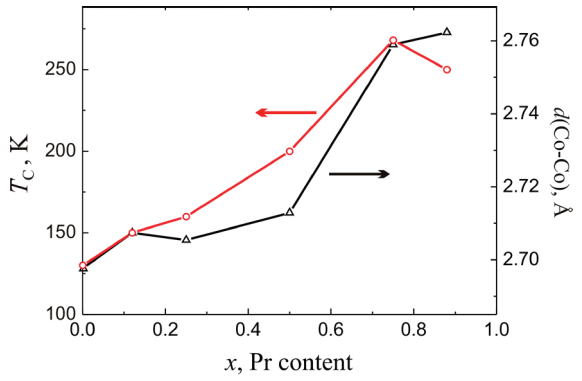

Figure 8. Variation of the intralayer Co−Co distance and ferromagnetic ordering temperature in $La_{1-x}Pr_xCo_2P_2$ as a function of Pr content, x. The standard deviations are smaller or comparable to the symbol size.

as occupied solely by La, since it is not possible to account for partial occupancies in LMTO.

Nonmagnetic Calculations. Both $LaCo_2P_2$ and $La_{0.12}Pr_{0.88}Co_2P_2$ exhibit a strong peak in the density of states (DOS) in the vicinity of the Fermi level (Figure S4). According to the Stoner criterion,[45] an itinerant magnet exhibits ferromagnetism when $In(E_F) > 1$, where I is a measure of the strength of metal exchange interaction, and $n(E_F)$ is the DOS at the Fermi level. In the first approximation, the values of I can be taken from the elemental metals.[46,47] According to our calculations, the $In(E_F)$ product equals to 1.6 and 3.1 for $LaCo_2P_2$ and $La_{0.12}Pr_{0.88}Co_2P_2$, respectively. Thus, the Stoner criterion indicates that both phases should exhibit ferromagnetic ordering. This correlates well with the ferromagnetic ordering of Co spins within the $[Co_2P_2]$ layer, as was established for $LaCo_2P_2$ and $PrCo_2P_2$ from neutron diffraction data. Note that such a DOS peak is also observed in the reported electronic structure of nonmagnetic $SrRh_2P_2$,[18] but it appears at ~0.2 eV above the Fermi level, which results in the much lower value of $In(E_F)$.

Dronskowski et al. demonstrated that the driving force for magnetic ordering lies in the local nonbonding or antibonding character of states in the vicinity of the Fermi level.[48] The crystal orbital Hamiltonian population (COHP) calculated along the shortest Co−Co distance of ~2.7 Å indicates a strong antibonding character of the Co−Co interaction within one layer (Figure S5). Thus, the nonmagnetic calculations support the possibility of spin polarization of the electronic structure and indicate the ferromagnetic type of nearest-neighbor interactions in $La_{1-x}Pr_xCo_2P_2$.

Magnetic Calculations. Calculations in the spin-polarized mode were performed assuming ferromagnetic ordering of all Co spins within the unit cell. This is a reasonable assumption, since all the studied La-containing $La_{1-x}Pr_xCo_2P_2$ phases ($0 \le x < 1$) exhibit ferromagnetic ordering

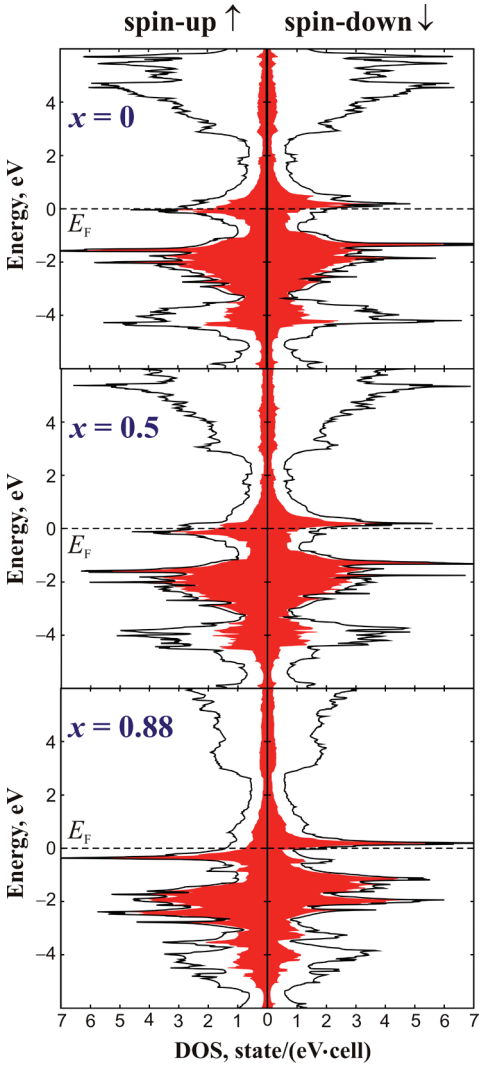

Figure 9. Spin-polarized DOS for $LaCo_2P_2$ (top), $La_{0.5}Pr_{0.5}Co_2P_2$ (middle), and $La_{0.12}Pr_{0.88}Co_2P_2$ (bottom). The Co 3*d* contribution is shown in red.

below room temperature. For $LaCo_2P_2$, the spin-up DOS resembles the nonmagnetic DOS, while the spin-down DOS is shifted to higher energies, thus providing the spin polarization expected for a ferromagnet (Figure 9). The difference between the spin-up and spin-down DOS channels below the Fermi level is 0.55 states/cell. A higher spin polarization is observed as the Pr content increases, and for $x = 0.5$ and 0.88 the difference between the spin-up and spin-down DOS is 0.78 and 1.42 states/cell, respectively. This is in accord with the stronger intralayer Co−Co exchange interaction that manifests itself in the increase of T_C and θ at higher values of x.

Thus, the ferromagnetism of the studied compounds arises because of the strong DOS peak at the Fermi level. This instability is removed by spin polarization, as the peak becomes nearly completely filled in the spin-up channel and remains essentially unoccupied in the spin-down channel. The trend is reflected particularly well in the spin-polarized DOS of $La_{0.12}Pr_{0.88}Co_2P_2$. Note, however, that our calculations were performed for a ferromagnetic model and are valid only for the analysis of

(45) Stoner, E. C. *Proc. R. Soc. London, Ser. A* **1938**, *165*, 372–414.
(46) Janak, J. F. *Phys. Rev. B* **1977**, *16*, 255–262.
(47) Gourdon, O.; Bud'ko, S. L.; Williams, D.; Miller, G. J. *Inorg. Chem.* **2004**, *43*, 3210–3218.
(48) Landrum, G. A.; Dronskowski, R. *Angew. Chem., Int. Ed.* **2000**, *39*, 1560–1585.

intralayer interactions. Indeed, despite the stronger intralayer ferromagnetic exchange for the higher values of x, the $La_{1-x}Pr_xCo_2P_2$ phases with $x = 0.75$ and 0.88 also exhibit stronger antiferromagnetic coupling between the layers due to the shorter interlayer separation.

Conclusion

As demonstrated in this work, the rare-earth cobalt phosphides with the $ThCr_2Si_2$-type structure can exhibit magnetic properties as rich as those observed earlier for the analogous rare-earth manganese silicides and germanides. While the limiting members of the $La_{1-x}Pr_xCo_2P_2$ series, $LaCo_2P_2$ and $PrCo_2P_2$, show rather simple magnetic behavior, phases with intermediate compositions exhibit multiple magnetic transitions, leading to the observation of metamagnetism and magnetic pole reversal. Furthermore, the ferromagnetic transition temperature of $LaCo_2P_2$ (132 K) increases dramatically upon substitution of Pr for La and reaches 268 K for $La_{0.25}Pr_{0.75}Co_2P_2$. This is in drastic contrast to the isostructural $La_{1-x}Pr_xMn_2Si_2$ phases, in which the ferromagnetic transition remains essentially unaffected by the substitution in the rare-earth sublattice. The temperature-driven ferro- and metamagnetic transitions observed in $La_{0.5}Pr_{0.5}Co_2P_2$ are accompanied by anomalous behavior of the unit cell parameters.

The increase in the ferromagnetic ordering temperature can be rationalized by the analysis of the calculated spin-polarized density of states, which reveals larger difference in the population of the majority and minority spin subbands for higher Pr content. This leads to stronger intralayer exchange interactions between the Co centers.

Despite the relatively large change in the unit cell parameters between $LaCo_2P_2$ and $PrCo_2P_2$, the magnetic behavior of the intermediate quaternary phases appears to be rather tolerant to the structural modifications, as a gradual change in the magnetic properties is observed with changing the La:Pr ratio. The observed magnetic and structural properties prompt investigation of the $La_{1-x}Pr_xCo_2P_2$ phases under high applied pressure and/or magnetic field, which might lead to detection of new magnetic or structural transitions. Establishing the exact nature of the observed magnetic transitions will require the use of neutron diffraction techniques. These studies, along with research on substitution of other rare earth metals into the $LaCo_2P_2$ structure, are currently underway, and their results will be reported in due course.

Acknowledgment. Florida State University is gratefully acknowledged for the financial support of this work. A special acknowledgment is made to the FSU Council on Research and Creativity for the PI Planning Grant for the startup of this project.

Supporting Information Available: Figures S1−S6 and Table S1. This material is available free of charge via the Internet at http://pubs.acs.org.